JMB

Available online at www.sciencedirect.com

ScienceDirect

ELSEVIER

Structural Studies on the Co-chaperone Hop and Its Complexes with Hsp90

S. C. Onuoha[1], E. T. Coulstock[1], J. G. Grossmann[2] and S. E. Jackson[1]*

[1]*Chemistry Department, Lensfield Road, University of Cambridge, Cambridge CB2 1EW, UK*

[2]*Molecular Biophysics Group, STFC Daresbury Laboratory, Daresbury Science and Innovation Campus, Daresbury, Warrington, Cheshire WA4 4AD, UK*

The tetratricopeptide repeat domain (TPR)-containing co-chaperone Hsp-organising protein (Hop) plays a critical role in mediating interactions between Heat Shock Protein (Hsp)70 and Hsp90 as part of the cellular assembly machine. It also modulates the ATPase activity of both Hsp70 and Hsp90, thus facilitating client protein transfer between the two. Despite structural work on the individual domains of Hop, no structure for the full-length protein exists, nor is it clear exactly how Hop interacts with Hsp90, although it is known that its primary binding site is the C-terminal MEEVD motif. Here, we have undertaken a biophysical analysis of the structure and binding of Hop to Hsp90 using a variety of truncation mutants of both Hop and Hsp90, in addition to mutants of Hsp90 that are thought to modulate the conformation, in particular the N-terminal dimerisation of the chaperone. The results establish that whilst the primary binding site of Hop is the C-terminal MEEVD peptide of Hsp90, binding also occurs at additional sites in the C-terminal and middle domain. In contrast, we show that another TPR-containing co-chaperone, CyP40, binds solely to the C-terminus of Hsp90.

Truncation mutants of Hop were generated and used to investigate the dimerisation interface of the protein. In good agreement with recently published data, we find that the TPR2a domain that contains the Hsp90-binding site is also the primary site for dimerisation. However, our results suggest that residues within the TPR2b may play a role. Together, these data along with shape reconstruction analysis from small-angle X-ray scattering measurements are used to generate a solution structure for full-length Hop, which we show has an overall butterfly-like quaternary structure.

Studies on the nucleotide dependence of Hop binding to Hsp90 establish that Hop binds to the nucleotide-free, 'open' state of Hsp90. However, the Hsp90–Hop complex is weakened by the conformational changes that occur in Hsp90 upon ATP binding. Together, the data are used to propose a detailed model of how Hop may help present the client protein to Hsp90 by aligning the bound client on Hsp70 with the middle domain of Hsp90. It is likely that Hop binds to both monomers of Hsp90 in the form of a clamp, interacting with residues in the middle domain of Hsp90, thus preventing ATP hydrolysis, possibly by the prevention of association of N-terminal and middle domains in individual Hsp90 monomers.

Edited by F. Schmid

Corresponding author. E-mail address: sej13@cam.ac.uk.

Introduction

Heat Shock Protein 90 (Hsp90) is an essential stress protein that is involved in the maturation and activation of a number of proteins, collectively known as clients. Many of these are involved in fundamental cellular processes such as transcriptional regulation, cell cycle regulation, and signal transduction.[1–4] A

large number of Hsp90 client proteins have been shown to be upregulated in cell cycle regulation and apoptosis pathways that are commonly deregulated in cancer.[5,6] Hsp90 has thus, despite its ubiquitous nature and importance for cellular viability, become a validated target for cancer therapeutics.[7] The Hsp90 inhibitor 17-AAG is currently in phase II clinical trials.[5]

Functionally, Hsp90 does not operate alone but is dependent on a cohort of co-chaperone proteins that interact at different stages along the pathway of client protein maturation in a manner that is dependent on ATP.[8] The assembly and functional maturation of steroid receptor complexes by the Hsp90 cellular assembly machine have been extensively studied and are well characterized.[1] In this pathway, the steroid receptor initially associates with Hsp40 and Hsp70; then, through an interaction between the Hsp-organising protein (Hop) with both Hsp70 and Hsp90, the receptor is passed on to Hsp90. ATP binding to Hsp90 results in the dissociation of Hop and subsequent interaction of other co-chaperones such as p23 and large peptidyl-prolyl isomerases such as FKBP52 or Cyp40; the specific prolyl isomerase is believed to be dependent on the steroid receptor client protein. Hydrolysis of ATP by Hsp90 is believed to result in further conformational changes that lead to activation of the client protein, in the case of steroid receptors to a high-affinity ligand-binding state.[9]

The co-chaperone Hop binds to both Hsp70 and Hsp90. Biochemical and co-crystallographic studies have shown that the EEVD-containing C-termini of Hsp70 and Hsp90 bind specifically to the Hop tetratricopeptide repeat domains, TPR1 and TPR2a, respectively.[10] Hop has been shown to be a dimeric molecule in solution and binds as a dimer to dimeric Hsp90.[11] The binding of Hop to Hsp70 has been demonstrated to be a more complex process, which is affected by the presence of Hsp90 and ATP. Truncation of the EEVD motif of Hsp70 does not inhibit the ability of Hop to co-immunoprecipitate with the protein.[11] Further to this, point mutations in TPR2a or TPR2b and DP2 have all been shown to have inhibitory effects on the binding of Hsp70 to Hop.[12–14] Crystal structures of the individual domains of Hop bound to Hsp70 and Hsp90 EEVD C-terminal peptides have been solved.[10] However, subsequent studies have demonstrated that mutations in regions of Hsp90 distant from the C-terminus of the protein affect the binding of Hop, indicating that Hop may interact with Hsp90 at multiple sites in order to facilitate client protein transfer from Hsp70.[15] While crystal structures of individual TPR domains of Hop have been published, no structural data are presently available for the full-length protein.

In this study, small-angle X-ray scattering (SAXS) is used in combination with biochemical data and modelled structures of individual domains of Hop to obtain a model for the structure of full-length Hop in solution. In addition, we investigated the effects that binding of both full-length Hsp90 and the Hsp90 C-terminal SRMEEVD peptide motif have on the conformation of Hop in solution in order to gain insight into how Hop facilitates the interaction between Hsp70 and Hsp90 and the transfer of client proteins to the latter. A series of truncation mutants of Hop were generated to investigate the dimerisation interface. Together, these data are used to produce a solution structure for Hop where the dimerisation interface is located in the TPR2a domain, consistent with recent results from other laboratories.[16] We found that binding of Hop reduces the conformational space that Hsp90 is sampling in solution, and that structural changes in Hop are induced on binding the C-terminal MEEVD peptide, which may then facilitate further interactions with other sites on Hsp90. Finally, we propose a mechanism by which Hop may aid the transfer of client proteins from Hsp70 to Hsp90.

Results

Hop interacts with the C-terminal and middle domains of Hsp90

The main interaction between human Hop and Hsp90 has been shown to occur between TPR2a (Fig. 1) of Hop and the C-terminal SRMEEVD motif of Hsp90.[10] However, it has recently been shown that mutations outside the C-terminal domain of Hsp90 also affect the binding affinity for Hop.[15] To investigate in detail the binding of Hop to Hsp90 compared to other TPR-containing co-chaperones, isothermal titration calorimetry (ITC) was used to measure the binding of various Hsp90 truncation mutants (Fig. 2) to full-length Hop and the TPR-containing co-chaperone Cyp40 (Fig. 3, Table 1). A series of truncation mutants of Hsp90, including full-length Hsp90, Hsp90MC (a construct containing middle and C-terminal domains only), Hsp90C (the C-terminal domain alone) and the TPR binding C-terminal peptide (SRMEEVD) (Fig. 2), were titrated into a cell containing full-length wild-type (WT) Hop. Data were fit with three floating variables: stoichiometry, association binding constant (K_{obs}), and the change in enthalpy of interaction. Full-length Hsp90 (Hsp90FL) was determined to bind to Hop with a dissociation constant, K_d ($1/K_{obs}$), of 0.69 (± 0.04) µM at a stoichiometry of 1.06 ± 0.05, indicating that Hop binds as a dimer to a dimer of Hsp90. A
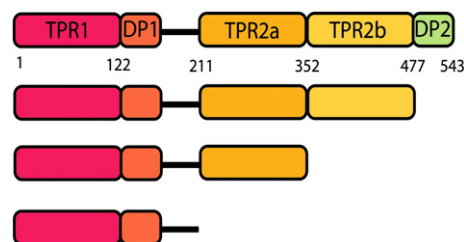
Fig. 1. Truncations of Hop were made that represented full-length Hop (1–543), Hop Δ DP2 (1–477) lacking the C-terminal aspartic acid proline (DP)-rich domain, Hop Δ TPR2b and DP2 (1–352) and Hop TPR1+DP1 (1–211).
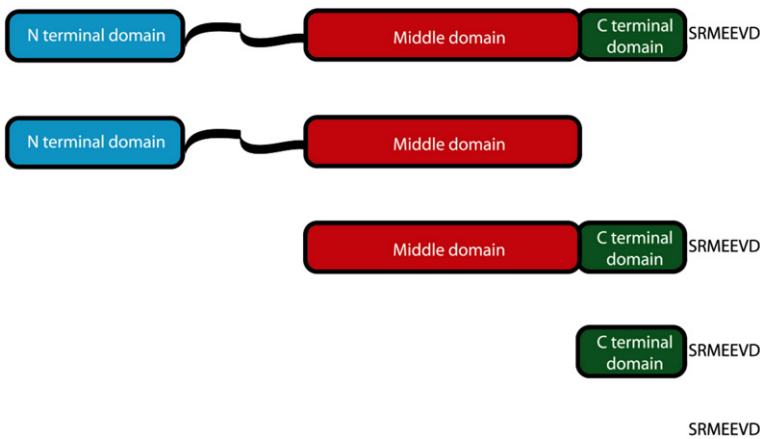
Fig. 2. Hsp90 truncations: (1) Hsp90FL, full-length Hsp90; (2) Hsp90ΔC, Hsp90 minus the C-terminal domain; (3) Hsp90MC, the middle and C-terminal domain of Hsp90; (4) Hsp90C, C-terminal domain of Hsp90 alone; (5) SRMEEVD, the C-terminal TPR-binding peptide.

construct consisting of the middle and C-terminal domains of Hsp90 (Hsp90MC) bound to Hop with a similar affinity, $K_d = 0.72$ (± 0.05) μM, at a stoichiometry of 0.9 ± 0.1. The C-terminal domain (Hsp90C) bound to Hop with a K_d of 4.3 (± 0.2) μM at a stoichiometry of 0.98 ± 0.06, whilst the C-terminal peptide alone bound to Hop with a K_d of 69 (± 3) μM at a stoichiometry of 1.00 ± 0.04. An Hsp90 construct consisting of the N-terminal and middle domains did not bind to Hop (data not shown). In order to investigate if the results seen were specific to Hop or true of all TPR-containing Hsp90-binding proteins, the binding of Cyp40 to Hsp90, Hsp90MC, Hsp90C and the SRMEEVD peptide was examined. In contrast to the results obtained for Hop, Cyp40 bound

to full-length Hsp90 with a similar affinity to that of the two truncation mutants and the C-terminal peptide (Table 1). In each case, the stoichiometry of binding was approximately 1:1, indicating that a monomer of Cyp40 binds per monomer of Hsp90. Taken together, these data confirm that the binding of Hop to Hsp90 is not only limited to the C-terminal TPR-binding peptide of the protein, but interactions elsewhere in Hsp90 are also involved. In agreement with these observations, titration of a truncation mutant of Hsp90 lacking the entire C-terminal domain, Hsp90ΔC, into a solution of Hop saturated with the SRMEEVD peptide resulted in a very weak binding interaction; however, this interaction was not strong enough to accurately
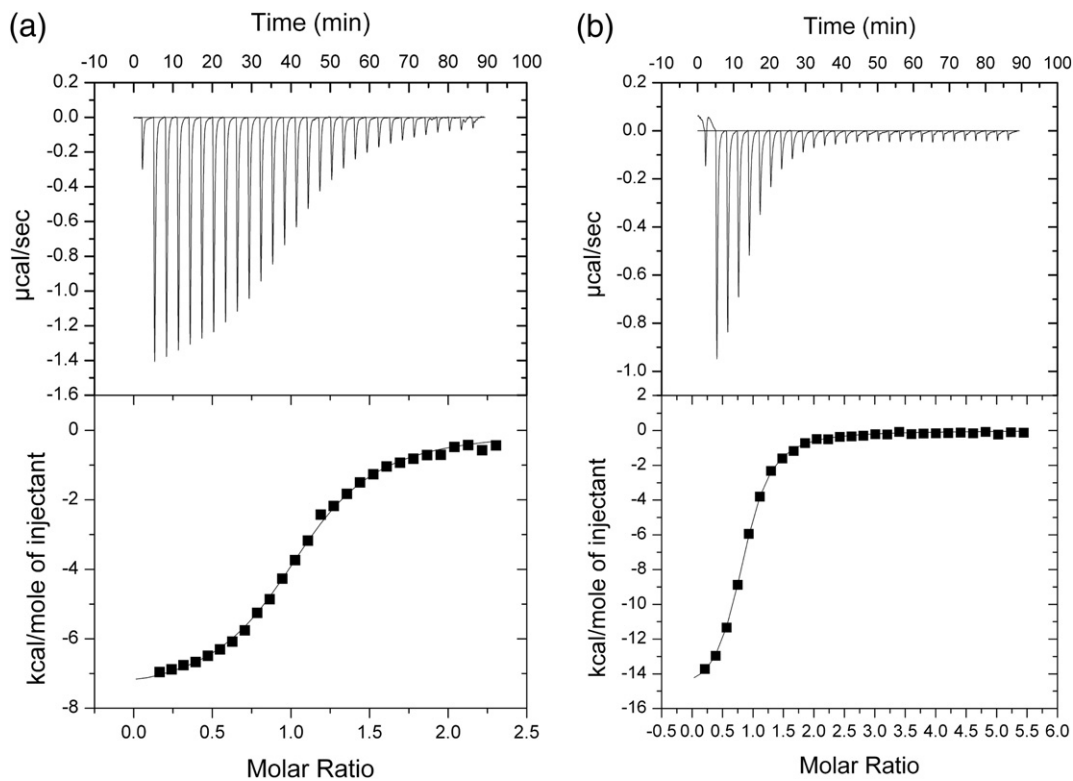
Fig. 3. Isothermal titration calorimetry experiment of the binding of wild-type Hsp90 to Cyp40 (a) and Hop (b). Hsp90 was injected into a cell containing Cyp40 or Hop. Both co-chaperones bound to Hsp90 with stoichiometries of approximately 1:1 and dissociation constants of 3.84 and 0.69 μM for Cyp40 and Hop, respectively.

Table 1. ITC measurements of Hsp90–co-chaperone interactions

Protein complex	Nucleotide	K_d (μ)M	ΔH (cal mol^{-1})	ΔS (cal mol^{-1} K^{-1})	N
WT Hsp90–Hop		0.69±0.04	13,260±126	−16.3	1.06±0.05
Hsp90MC–Hop		0.72±0.05	−8276±185	−0.06	0.90±0.1
Hsp90 C–Hop		4.3±0.2	−10,360±152	−10.2	0.98±0.06
SRMEEVD–Hop		69±3	−9981±477	−15.9	1.00±0.04
WT Hsp90–Cyp40		3.84±0.29	−7143±57	0.82	1.05±0.01
Hsp90MC–Cyp40		3.48±0.21	−7638±74	−0.65	1.06±0.01
Hsp90C–Cyp40		4.8±0.22	−5978±51	4.29	1.10±0.01
SRMEEVD–Cyp40		12.3±0.7	−6628±122	0.24	0.99±0.02
Hsp90WT–Hop	AMPPNP	0.65±0.02	−15,570±120	−23.7	0.91±0.04
Hsp90A116N–Hop	AMPPNP	2.2±0.1	−12,230±221	−15.0	1.28±0.16
Hsp90A116N–Hop		0.62±0.08	−14,270±203	−19.2	1.25±0.13
Hsp90T110I–Hop	AMPPNP	0.71±0.09	10,370±179	−6.65	1.23±0.10
Hsp90T110I–Hop		0.67±0.06	−11,580±239	−11.5	1.22±0.02

Isothermal titration calorimetry was used to investigate the interaction between Hsp90 truncation mutants and the TPR-containing co-chaperones Hop and Cyp40. WT Hsp90 is full-length human Hsp90β, Hsp90MC is a construct containing the middle and C-terminal domains only, Hsp90C is a construct containing the C-terminal domain only and SRMEEVD is a peptide corresponding to the last seven residues of human Hsp90β. The interactions between Hop and Hsp90 temperature-sensitive mutations were further investigated in the absence and presence of the ATP analogue AMPPNP. All experiments were carried out in 50 mM Tris, pH 7.4, 6 mM MgCl$_2$, 20 mM KCl and 1 mM tris(2-carboxyethyl)phosphine at 25 °C.

determine a dissociation constant using ITC (data not shown).

In order to investigate the effect of nucleotide binding on Hop interactions with Hsp90, ITC experiments were carried out on WT Hsp90 and the mutants A116N (A107N in yeast Hsp82) and T110I (T101I in yeast Hsp82). A107N has been shown in yeast to stabilize N-terminal dimerisation in the presence of the ATP analogue AMPPNP,[17–19] while T101I is believed to reduce N-terminal dimerisation and thus ATP hydrolysis.[17,19] Wild-type Hsp90 bound to Hop with similar K_d values in the absence and presence of AMPPNP, 0.69 (±0.04) and 0.65 (±0.02) μM, respectively (Table 1). The T110I mutant also bound to Hop with similar binding affinities in the absence and presence of nucleotide, 0.9 (±0.09) and 0.67 (±0.06) μM, respectively. In contrast, the A116N mutant bound to Hop with a reduced affinity in the

presence of AMPPNP, $K_d = 2.2$ (±0.1) μM, compared to the nucleotide-free state, $K_d = 0.62$ (±0.08) μM.

The TPR2a domain contains the dimerisation interface

In order to investigate the domains necessary for dimerisation of Hop, a series of truncation mutants of the protein were generated (Fig. 1) and analyzed using analytical size-exclusion chromatography (SEC) and SAXS. The oligomeric states of full-length Hop and Hop truncations were examined using SEC at various concentrations of protein between 3.25 and 100 μM. Data throughout this concentration range suggested that full-length Hop and the 1–211 truncation mutant formed dimeric and monomeric species, respectively (Table 2). At concentrations

Table 2. Size and shape determination of Hop truncations and Hsp90–co-chaperone complexes using SEC and SAXS

Protein	Calculated molecular mass (SEC) (Da)	R_g (Å)	D_{max} (Å)
Hop pH 7.4	141,000	55.2±0.3	193
Hop pH 5.0		54.8±0.4	191
Hop 1–211	32,000	27.5±0.1	85
Hop 1–352 (50 μM)	77,000	41.8±0.3	136
Hop 1–352 (5 μM)	48,000	32.6±0.2	
Hop 1–477	121,000	52.1±0.5	189
Hop-SRMEEVD		51.1±0.4	175
Hsp90		62.2±1	207
Hsp90–Hop		61.5±0.5	204
Cyp40	25,000	30.5±0.5	108
Hsp90–Cyp40	392,000	63.5±1	210

Hsp90, Cyp40, Hop, Hsp90 co-chaperone complexes and Hop truncations were analyzed using SEC and SAXS. Following standard curve generation using molecular mass standards, molecular weights were calculated based on the retention volume of the proteins and complexes. Radius of gyration (R_g) values were calculated using the indirect Fourier transform method and confirmed by analyzing the very low angle profiles using Guinier analysis (see Materials and Methods).
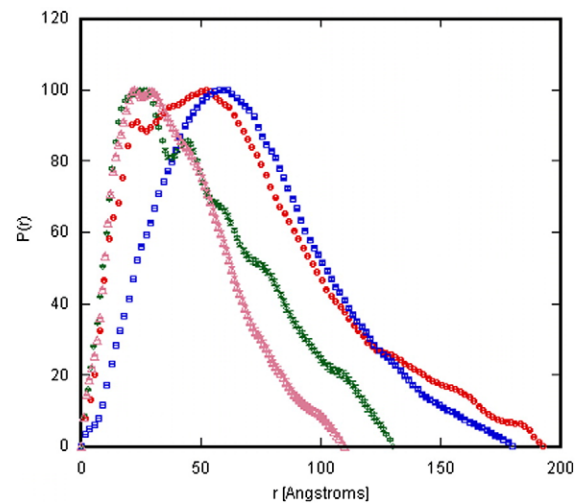
Fig. 4. Determination of the oligomeric status of Hop truncations using SAXS. P(r) functions deduced from scattering profiles were obtained for wild-type Hop (red ○), Hop 1–477 (blue □), Hop 1–352 (green ◊) and Hop 1–211 (pink △).

above 50 µM, the 1–352 mutant eluted at a volume consistent with that of a dimeric molecule. However, at lower concentrations a shift in the elution profile was observed, suggesting that the molecule exists as a mixture of monomeric and dimeric species (Table 2).

SAXS was used to obtain further information on the structure of the Hop dimer in solution. This technique is valuable for structural analysis of proteins in solution (albeit at low resolution) if structural details of individual domains are known. It is well known that the SAXS pattern is sensitive to the size and shape of a scattering molecule; the former can be estimated using the radius of gyration (R_g) along with its maximum diameter (D_{max}).[20] SAXS measurements of full-length and truncated Hop

variants were carried out to investigate the oligomeric state of the protein in solution. Comparing the relative I_0 with proteins of known molecular mass and concentration (Fig. 4 and Table 2), our results clearly indicate that full-length Hop exists in solution as a dimer, consistent with literature results.[1,21,22] Hop was shown to be dimeric at all concentrations studied (down to 5 µM). As observed in the SEC experiments, SAXS experiments showed that the 1–477 truncation was dimeric. The radius of gyration obtained (52.1 ± 0.5 Å) signifies a relatively modest reduction in overall size compared to WT. The 1–352 truncation gave a scattering profile indicative of a dimeric molecule at concentrations above 50 µM; however, at lower concentrations (below 5 µM) a reduction in the R_g was seen, suggesting a dynamic
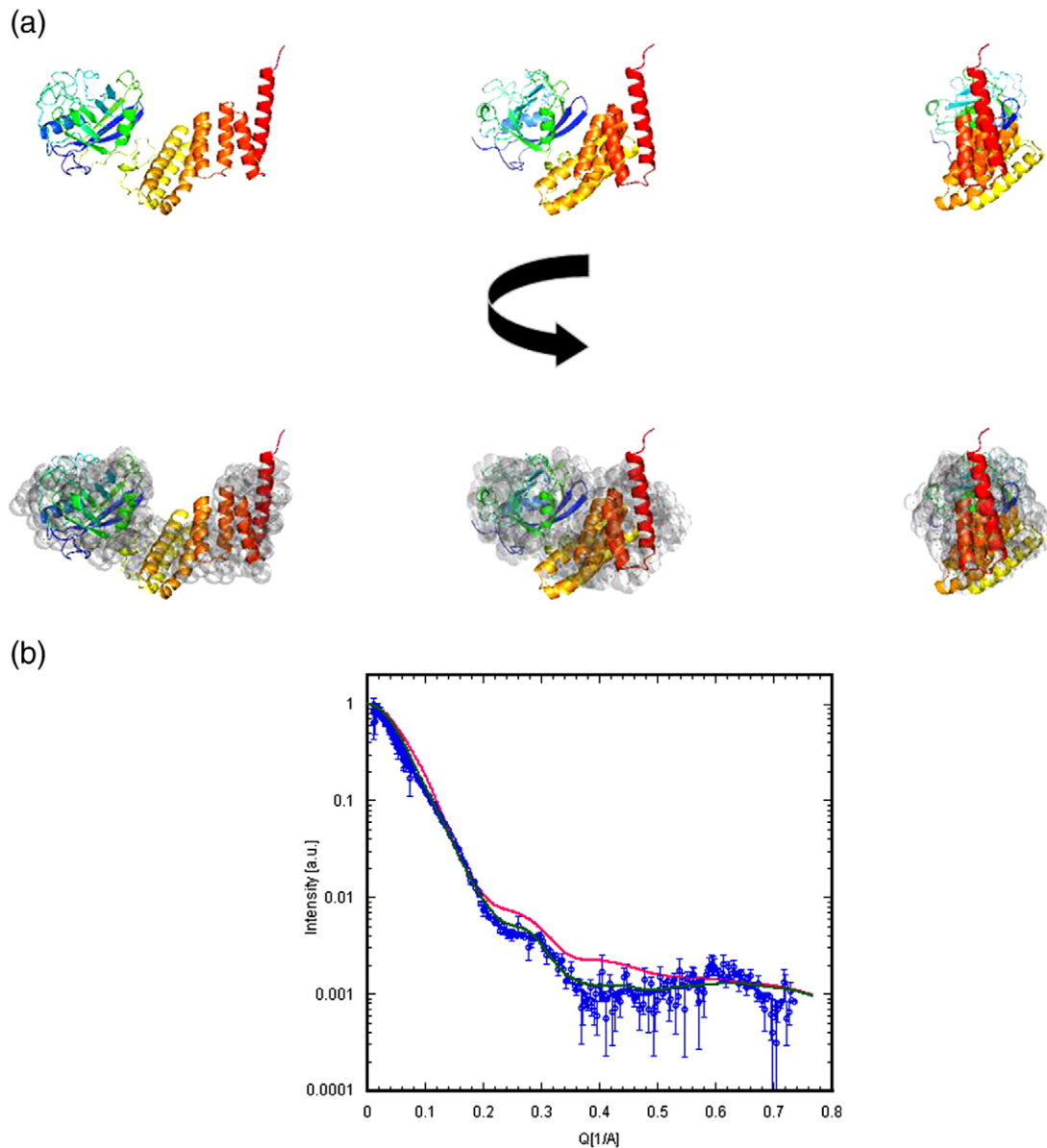
Fig. 5. (a) Solution structure of Cyp40. Following GASBOR reconstruction from raw data, the X-ray crystal structure of the monoclinic form of Cyp40, shown in cyan, was aligned with the *ab initio* SAXS reconstruction using the program SUBCOMP. (b) The scattering profile of Cyp40 (blue ○) was compared to the theoretical scattering profile of the crystallized monoclinic (green fit) and tetragonal (red fit) forms of Cyp40, using the package CRYSOL.

equilibrium. The 1–211 truncation gave a scattering profile consistent with that of a monomer (Fig. 4). Taken together, the data suggest that the second TPR domain, TPR2a, is responsible for the dimerisation of Hop, consistent with recently published work from Flom *et al.* on the yeast homologue Sti1.[16] However, it would appear that TPR2b also plays some role in the monomer–monomer interaction of the full-length molecule.

Ab initio shape reconstruction of co-chaperones and investigation of their interactions with Hsp90

SAXS experimental data were collected at protein concentrations of 10 and 1 mg/mL at camera-to-detector distances of 1 and 5.25 m, respectively, for both TPR-containing co-chaperones, Hop and Cyp40. The two data sets were merged and used for *ab initio* shape reconstruction (see Materials and Methods). Cyp40 is monomeric in solution, yet has been crystallized in two forms, a monoclinic and a tetragonal form, which have different conformations in their TPR domains.[23] The shape reconstruction agrees well with the conformation in the monoclinic crystal form (Fig. 5b), confirming that Cyp40 in solution exists in this state[23,24], suggesting that the observed structure of the tetragonal crystal form is likely to be a crystallographic artifact. The scattering profiles obtained experimentally were compared to theoretical scattering curves for the two elucidated
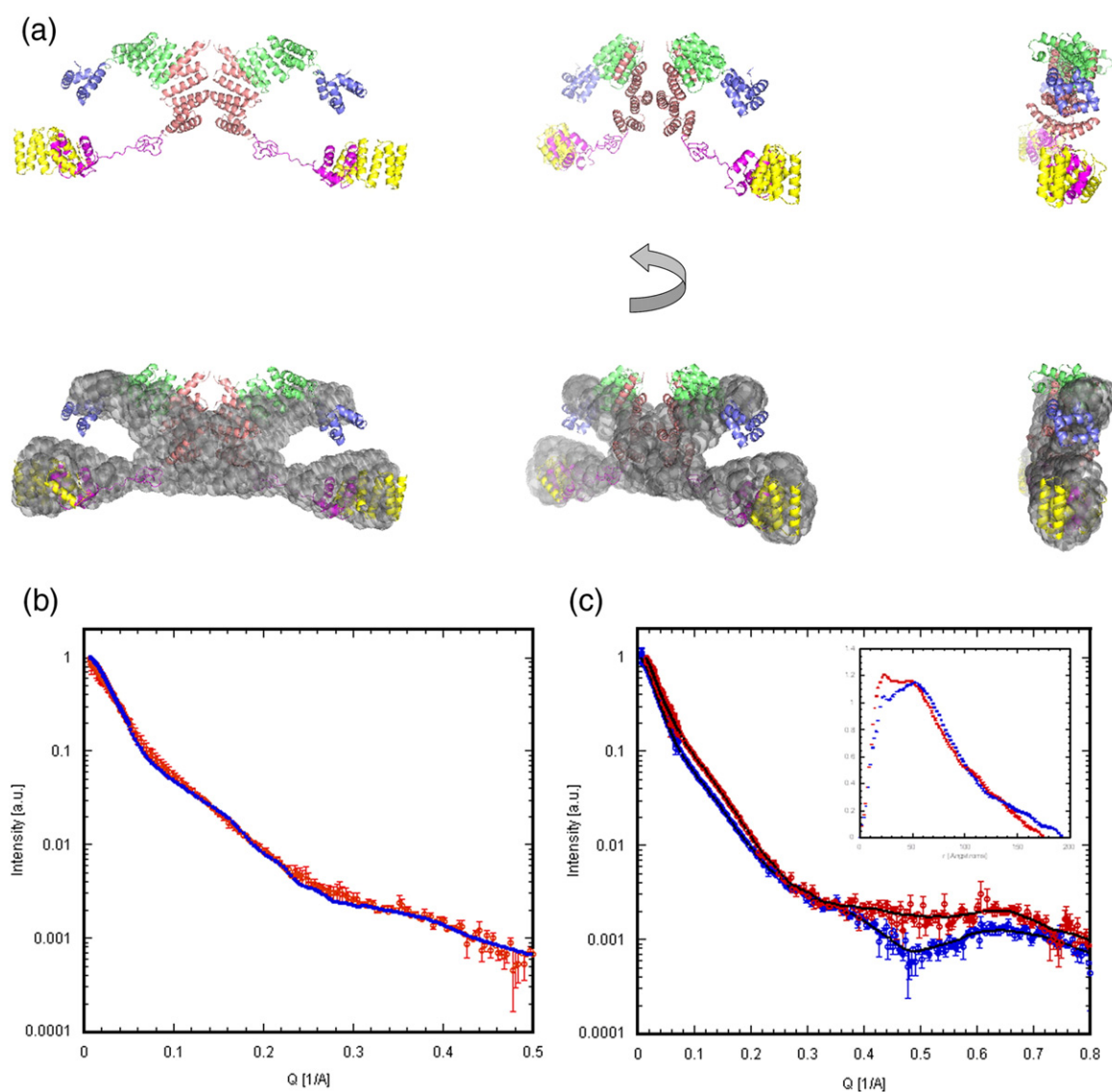
Fig. 6. (a) Solution structure of Hop following GASBOR reconstruction. Rigid-body modeling of the individual domains of Hop was carried out using the program BUNCH and aligned using SUBCOMP. (b) The experimental data for WT Hop (red ○) compared with the theoretical fit for the modeled structure obtained with BUNCH, shown in blue. (c) Scattering profile of Hop in the absence (blue ●), and presence (red ●) of the C-terminal SRMEEVD peptide. The $p(r)$ *versus* r plot inset shows clearly that not only is the D_{max} of the protein affected but that protein also adopts a significantly different conformation. (d) Solution structure of peptide-bound Hop following GASBOR reconstruction. Peptide-bound Hop is shown in wheat, superimposed over the solution structure of full-length Hop in the absence of peptide (shown in grey).

(d)
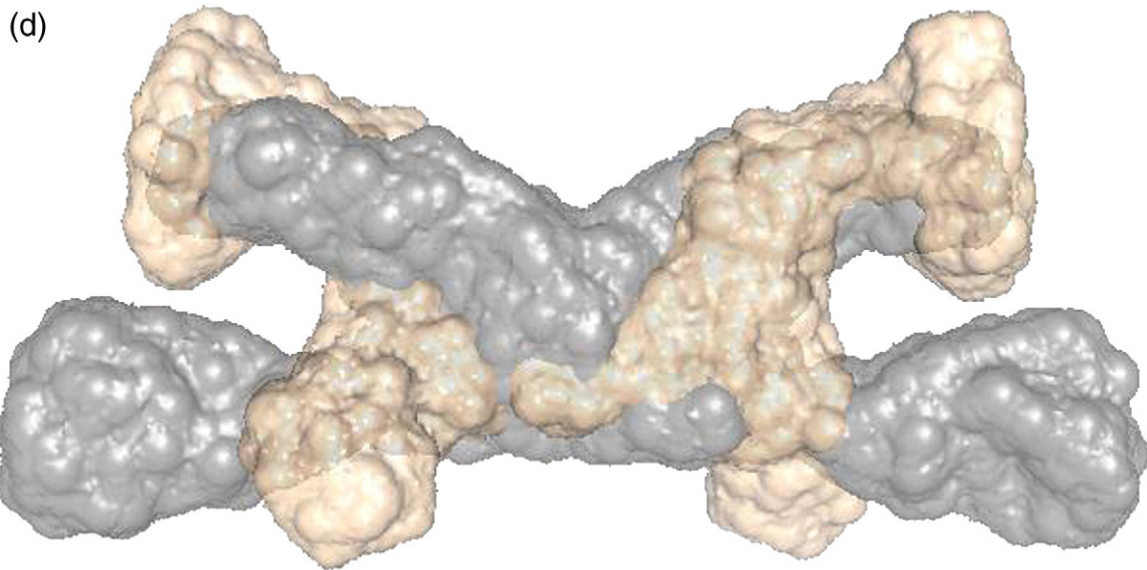
Fig. 6 (*legend on previous page*)

crystal structures using CRYSOL.[17] Chi-square values between theoretical and experimentally obtained data further confirmed that the solution structure of Cyp40 fit best the monoclinic crystal structure (Fig. 5b).

To date, no crystal structure exists for full-length Hop. Shape reconstructions of WT Hop were carried out using a 2-fold symmetry constraint emphasizing the dimeric nature of the molecule in solution (Fig. 6a). In addition, the primary dimerisation interface of Hop has been shown to be located at TPR2a,[16] with some contribution likely from TPR2b. Using the crystal structures of TPR1 and TPR2a and by using a homology model for TPR2b as well as predicted structures for DP1 and DP2 (generated using the protein structure prediction server Lomets[25]) we performed rigid-body modeling of the domains of Hop with the program Bunch (Fig. 6b). The dimer interface was assessed by considering another TPR-containing dimeric molecule of similar size and shape to Hop, the GlcNac protein.[26] The full-length rigid-body model of Hop agreed well with the *ab initio* shape obtained. Figure 6a shows our model of full-length Hop consistent with SAXS, protein engineering and SEC results. The radius of gyration of free Hop was calculated to be 54 Å. In the presence of the C-terminal SRMEEVD peptide, the R_g of Hop fell from 54±0.8 Å to 51±0.7 Å (Fig. 6c, Tables 1 and 2), suggesting that the interaction between the C-terminal peptide of Hsp90 and Hop induces a significant structural change in Hop. The solution structure of Hop bound to the SRMEEVD peptide generated using shape reconstructions with GASBOR is shown in Fig. 6d, superimposed on the *ab initio* model of Hop in the absence of peptide using the program SUBCOMP.

Interactions between Hop and Hsp90 were investigated using SAXS and SEC (Table 2, Fig. 7). Human Hop was shown, using SEC, to form a stable com-

plex with Hsp90, which elutes slightly earlier than Hsp90 alone. SAXS measurements of Hop, Cyp40, Hsp90, and complexes between Hsp90 and the two co-chaperones were carried out. The R_g and D_{max} values were calculated from the scattering profiles of these proteins and protein complexes (Table 2, Fig. 8). The R_g of free Hsp90 was 62±1 Å, whilst that of free Hop was 54±0.8 Å. Upon complex formation with Hop, the overall radius of gyration fell slightly to 61.5±1 Å. In contrast to this, the smaller co-chaperone Cyp40 binding to Hsp90 is accompanied by a significant increase in the overall R_g of the molecule, to 64±1 Å. These data are consistent with results obtained by SEC and suggest that binding of
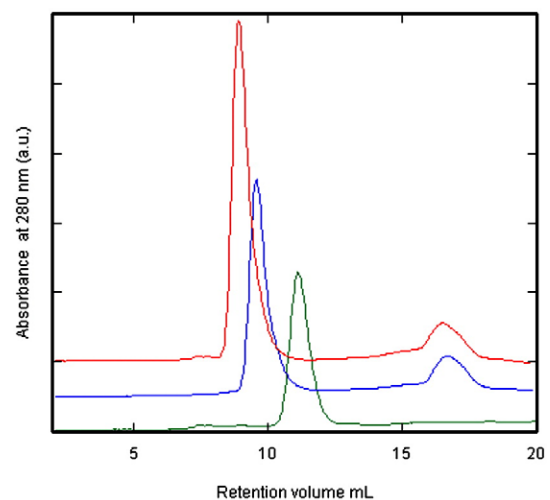
Fig. 7. Hop–Hsp90 complex formation as observed with SEC. (1) Hsp90 (blue), (2) Hop (green) and (3) equal concentrations of Hop and Hsp90 (red) were analyzed by SEC.
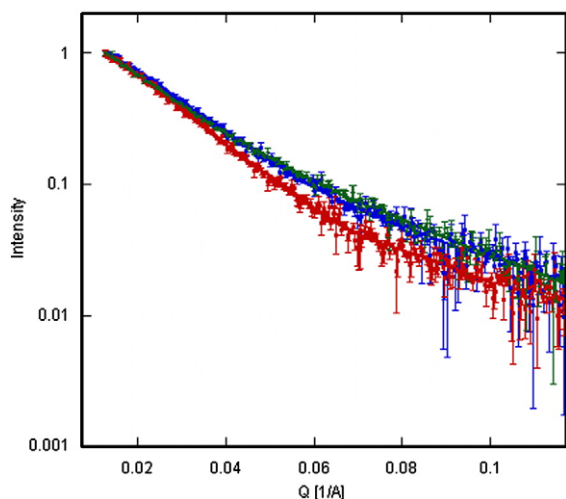
Fig. 8. SAXS of Hsp90 (blue ●) and the Hsp90–Cyp40 (green ♦) and Hsp90–Hop (red ■) complexes.

Hop to Hsp90 restricts the overall conformational flexibility of the Hsp90 dimer.

Discussion

In this study, we have used SAXS in combination with biochemical analysis to establish solution structures for two co-chaperones of Hsp90, Hop and Cyp40, and investigated their interactions with Hsp90. It has previously been shown that regions outside of the MEEVD-containing C-terminal domain of Hsp90 are important for binding between Hsp90 and Hop.[10] Our results agree well with these findings. Using ITC, we have shown that Hop has a 100-fold greater affinity for full-length Hsp90 than the SRMEEVD peptide alone. Interestingly, we observed that while no binding was evident between Hop and a truncation mutant of Hsp90 lacking the C-terminal domain, Hsp90ΔC, in the presence of saturating quantities of the C-terminal peptide, weak binding between Hop and Hsp90ΔC did occur. This suggests that binding of the C-terminal peptide of Hsp90 to Hop may induce conformational changes in the co-chaperone that expose residues that are important in the binding of Hop to areas outside the C-terminal domain of Hsp90. Hop bound to Hsp90MC, a construct of Hsp90 containing only the middle and C-terminal domains, with a similar affinity to that of full-length Hsp90, suggesting that interactions between Hop and Hsp90 are limited to the middle and C-terminal domains. In contrast to Hop, Cyp40 bound to Hsp90 and both the isolated C-terminal domain and the Hsp90 MC construct with similar affinities. Binding to the SRMEEVD peptide was reduced twofold in comparison to the C-terminal domain, suggesting that, while not limited to the SRMEEVD peptide, Cyp40 interacts solely at the C-terminus of Hsp90.

A recent study has suggested that the minimal fragment of Hop required for dimerisation is the Hsp90-binding TPR2a domain.[16] Using a combination of SEC and SAXS, we have shown here that TPR2a does indeed contain the major dimerisation interface: truncation mutants of Hop lacking TPR2a being monomeric, whilst those in which TPR2a was present gave elution and scattering profiles characteristic of dimers in both SEC and SAXS experiments. However, the Hop truncation mutant 1–352 lacking the TPR2b domain is only dimeric at high concentrations of protein, suggesting that there is an additional, but weaker, interaction site located in this domain.

The solution structures of Hop and Cyp40 were investigated using SAXS. The crystal structure of Cyp40 has been shown to exist in two forms.[27] It has been suggested, however, that the tetragonal form of the molecule may not exist in solution and that the characteristic elongated helix may actually be an artifact of crystallization.[24] Here, we have shown clearly that the solution structure fits more closely to the structure of the monoclinic crystal form confirming this hypothesis (Fig. 5a). Having used the method of *ab initio* shape reconstruction to elucidate the solution structure of a co-chaperone of which the crystal structure had been solved, we set about the more challenging task of attempting to use SAXS data to reconstruct the shape of the larger Hop co-chaperone for which, to date, no crystal structure exists. With knowledge of the domain structures and locations in Hop, and having determined the dimerisation interface of the molecule, we have modeled the crystal structures of the two TPR domains previously solved,[10] a homology model of TPR2b as well as predicted structures for DP1 and DP2 into the reconstructed molecular envelope, to obtain a model of Hop in solution. Shape reconstructions of Hop consistently yielded a 'butterfly' shape (Fig. 6a).

Conformational changes that accompany the binding of Hsp90 to the co-chaperones Hop and Cyp40 were also investigated using SAXS (however, this was only performed at low scattering angles, which does not allow a detailed shape analysis). Upon binding, Hsp90 and Cyp40 formed a complex with an overall R_g larger than that of Hsp90 alone; these data agreed well with results obtained by ITC, suggesting that the Cyp40 binds to Hsp90 at one site at the C-terminus of the protein, and are also in keeping with the observation that binding of Cyp40 has no effect on the ATPase activity of Hsp90.[28] It should be noted that unlike Hop, a complex between Cyp40 and Hsp90 that did not dissociate upon progression through a size-exclusion column could not be obtained. A small peak eluted at a position corresponding to Cyp40 (data not shown). A free component in solution during the SAXS experiments would contribute to the overall scattering intensity. If significant amounts of free Cyp40 were present, a reduction in the overall R_g would be observed. Instead an increase in size is measured, suggesting that although the complex was not stable enough to withstand passage through a size-exclusion column, it remained intact over the course of the SAXS experiment.

In contrast to Cyp40, Hsp90 and Hop formed a stable complex with a rather smaller R_g than Hsp90 alone. This suggests that Hop binds to Hsp90 and limits the conformational space that a free multi-domain Hsp90 would normally sample in solution. Interestingly, binding of the SRMEEVD peptide to Hop also reduced the R_g of Hop. The binding of Hop to the Hsp90 SRMEEVD peptide has been previously shown to induce conformational changes resulting in domain–domain interactions in Hop.[29] Shape reconstruction of Hop in the presence of SRMEEVD appears to suggest that TPR1 and DP1 domains come closer together, although the exact nature of the interactions that occur upon Hop–SRMEEVD binding remain speculative; it is possible to suggest that when Hop binds to the C-terminal SRMEEVD motif of Hsp90 a conformational change is induced in Hop, potentially causing the molecule to close around Hsp90 in the form of a clamp, restricting the dynamics of the molecule and/or exposing residues in Hop that are responsible for additional interactions outside the C-terminal domain of Hsp90. Here, we have shown that physical interactions between Hop and Hsp90 are limited to the middle and C-terminal domains. Interestingly, in our proposed model of Hop the distance between the Hsp90-binding site in the molecule and the C-terminal helix in DP2 is about 80 Å, which is smaller than the distance between the C-terminus of Hsp90 and the beginning of the charged linker region of the protein, which measures 85 Å,[17] suggesting strongly that Hop cannot interact directly with the N-terminal domain of Hsp90. TPR2b is essential for Hsp90 binding[13,30]; it is possible that Hop may interact with Hsp90 initially via TPR2a and clamp around Hsp90 via TPR2b and DP2. As discussed later, these movements may have implications in Hsp70–Hop binding. Deletion of the C-terminal DP2 domain has a relatively small effect on the radius of gyration, suggesting that as depicted in the shape reconstruction this domain is unlikely to project into solution and probably approaches TPR1. If this domain was located at the periphery of Hop one would expect a larger influence on the scattering profile as a result of a significant reduction in molecular size of the C-terminally truncated Hop lacking DP2.

The yeast homologue of Hop, Sti1, has been shown to inhibit the ATPase activity of yeast Hsp82,[28,31] and whilst human Hop has no effect on the lower basal ATPase activity of human Hsp90, it does inhibit the client-stimulated ATPase activity of the protein.[32] The effects of mutations that influence N-terminal dimerisation in Hsp90 on Hop binding have been studied with conflicting results. Johnson *et al.*[15] showed that mutations in the constitutively expressed yeast Hsc82 favoring N-terminal dimerisation inhibited Sti1–Hsc82 interactions in the presence of nucleotide, whilst mutations that reduced N-terminal dimerisation interacted in a manner similar to that of WT Hsc82. In contrast, Siligardi *et al.*[33] showed that purified Sti1 did not exhibit any reduced interaction with equivalent mutants in the yeast heat-shock-inducible analogue, Hsp82. Due to

the discrepancy in the observed effects of this set of mutations, it has been questioned whether the effects seen were isoform specific or indeed reproducible in experiments using purified protein. Here, we have probed the effect of these mutations on Hop binding using the human homologues. Ala116 in human Hsp90 is located within the lid segment that closes over the mouth of the nucleotide-binding pocket. In yeast, a mutation at the corresponding residue (A107N) exhibited enhanced N-terminal dimerisation and ATPase activity,[17,19] whilst T101I (T110I in human Hsp90) has been shown to disrupt N-terminal dimerisation. Here, we have shown that WT and both A116N and T110I mutants bind to Hop with similar affinities in the absence of the ATP analogue AMPPNP, A116N binding to Hop in the presence of nucleotide is slightly reduced, whilst T110I binding is unaffected by the presence of AMPPNP. As all experiments in this study were carried out using human Hsp90, it is clear that the results are not specific to yeast Hsc82, and are reproducible in experiments using purified proteins. Our data are consistent with a model in which Hop binds to the nucleotide-free 'open' state of Hsp90. This interaction, however, is weakened by the conformational changes that occur in Hsp90 upon ATP binding. The fact that Hop binding to Hsp90 in the presence of AMPPNP is unaffected, and even binding to the A116N mutant is merely reduced and not abolished, highlights the transient nature of any N-terminal dimerisation in human Hsp90 in the absence of a stabilizing factor such as the co-chaperone p23.

It has been shown that the mutations W277A and F325A in the middle domain of yeast Hsc82 reduce the interaction between Sti1 and Hsc82. The crystal structure of full-length Hsp90 bound to AMPPNP and the co-chaperone p23 has recently been solved.[17] The structure shows that upon nucleotide binding the N-terminal and middle domains of each Hsp90 monomer interact extensively, and that this interaction is stabilized by the packing of Phe200 into a hydrophobic pocket formed by Pro273, Trp277, Phe292 and Tyr344. Studies showing that Hop binding is disrupted by the mutation W277A indicate that Hop interacts with this residue. It is thus likely that binding of Hop to this site prevents the interaction between the middle and N-terminal domains of Hsp90 observed in the structure of the Hsp90–p23 complex. This interaction is essential for the catalytic residue (Arg380 in the yeast homologue) to interact with the γ-phosphate of ATP during ATP hydrolysis and explains the inhibitory effect that Hop/Sti1 has on the ATPase activity of Hsp90. Burial of Trp277 upon N-terminal dimerisation, as favored by mutations such as A116N, may deprive Hop of an important second binding site, leading to a reduced affinity as observed in this study. The fact that results presented here show that Hop does not directly interact with the N-terminal domain of Hsp90 suggest that this is the likely mechanism by which Hop inhibits ATP hydrolysis.

By analyzing co-evolving amino acids between Hsp70, Hop and Hsp90, Travers and Fares[34] demonstrated that it may be possible to obtain, *a priori*, information on interacting regions between proteins. Functional residues within TPR1 and TPR2A were shown to interact with Hsp70 and Hsp90, respectively. Several other residues were also identified, including some of those discussed in this study as being important for the interaction of Hop with Hsp90. Interestingly, other residues in Hop were
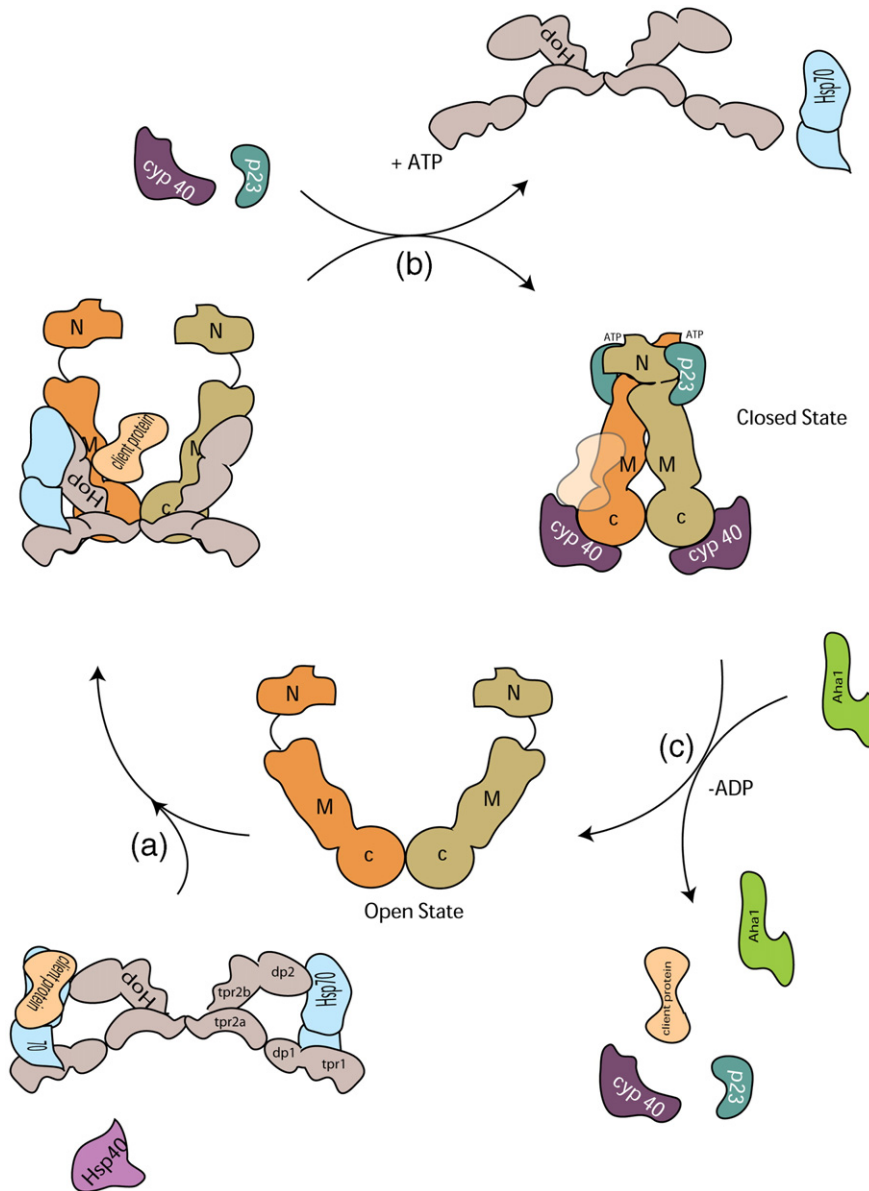
Fig. 9. Model of the conformational cycle of Hsp90. (a) In the initial step, the open form of Hsp90 is charged with a client protein; data from this study suggest that Hop may help present the client protein to Hsp90 by aligning the bound client and Hsp70 with the middle domain of Hsp90. TPR1 and DP2 appear to approach one another in the solution structure, providing a mechanism in which both domains bind to Hsp70. Dimeric Hop may bind to both monomers of Hsp90 through the TPR2b and DP2 domains, in the form of a clamp, interacting with the residues in the middle domain of Hsp90 and preventing ATP hydrolysis (one way in which this may occur is by the prevention of association of N and middle domains in individual Hsp90 monomers). The conformational changes that occur when Hop binds to Hsp90 may be responsible for the change in stoichiometric ratio between Hsp70 and Hop in the absence and presence of Hsp90, as previously described.[36] (b) Upon ATP binding to Hsp90, the Hsp90–Hop complex is weakened and, together with the binding of other co-chaperones such as large immunophilins such as Cyp40 or p23, Hop is displaced from the Hsp90 complex. Binding of ATP to Hsp90 then triggers conformational changes in the N and M domains ultimately resulting in N-terminal dimerisation and formation of a closed state, with composite active sites being formed between N and M domains of the same monomer. This closed state is further stabilized by p23. (c) The cycle is completed by hydrolysis of ATP that may be triggered by release of Hop or binding of client or Aha1 resulting in the activation and subsequent release of the client protein and restoration of the open state of Hsp90.

also shown to co-evolve with residues in Hsp90 and Hsp70 including residues in TPR2b and the DP2 repeat region, consistent with our results that show that residues in these domains also contribute to Hsp90 binding. Co-evolution of amino acids does not necessarily indicate that these residues interact with Hsp90/Hsp70 directly, and further work needs to be carried out in order to investigate the exact role these residues play in any interaction between Hop and Hsp70/Hsp90.

The binding of Hop to Hsp70 has long been predicted to occur via TPR1.[10,35,36] Indeed it has been shown that binding to mutations in TPR1 inhibit Hsp70 binding to Hop[11] as does deletion of the TPR1 domain. Paradoxically, the distant DP2 domain also appears to be involved and is essential for Hsp70–Hop interactions.[12,14] Here a model of the structure of full-length Hop is presented (Fig. 6a). Rigid-body modeling of Hop domains based on our solution scattering data suggests that TPR1 and DP2 domains may approach one another; it is thus possible that Hsp70 is able to bind to both DP2 and TPR1 simultaneously, explaining why previous studies have shown a necessity for both domains in Hsp70 binding.[37] The number of Hsp70 binding sites on the Hop dimer goes from two in the absence of Hsp90 to one in its presence.[37] The conformational changes that occur upon Hsp90 binding may occlude one of the Hsp70 binding sites. Studies on the nucleotide dependence of binding of Hop to Hsp90 establish that Hop binds to the nucleotide-free, open state of Hsp90. However, this complex is weakened by the conformational changes that occur in Hsp90 upon ATP binding. Together, the data are used to propose a detailed model of how Hop may help present the client protein to Hsp90, by aligning the bound client on Hsp70 with the middle domain of Hsp90 (Fig. 9). It is likely that Hop binds to both monomers of Hsp90 in the form of a clamp, interacting with residues in the middle domain of Hsp90 and thus preventing ATP hydrolysis, possibly by the prevention of association of N-terminal and middle domains in individual Hsp90 monomers.

Materials and Methods

Protein expression and purification

Human Hsp90β, the human Hsp90β mutants A116N and T110I, and Hsp90βΔC were expressed and purified as previously described.[38] Human Hsp90β C-terminal domain and Hsp90β MC were produced by subcloning the DNA corresponding to residues 546–724 and 274–724 of human Hsp90β into a pET28a expression vector containing an hexahistidine tag, and purified as previously described for Hsp90β.[38] Human Hop was expressed in a pET28a intein-CBD expression vector. Hop truncations were made by the introduction of a HindIII restriction site at the desired locations using site-directed mutagenesis (QuikChange, Stratagene). Plasmids were then cut with the appropriate restriction enzymes; the fragment corresponding to the truncated gene gel was purified and relegated into the parent pET28a vector using standard

molecular biology techniques. All expression vectors for the truncation mutants were sequenced to ensure the correct truncated gene was present. Full-length Hop and truncation mutants were purified as intein fusion proteins by passage through a chitin Sepharose column. CBD tags were cleaved overnight in the presence of 50 mM DTT. The eluted untagged proteins were purified on a mono Q HR10/10 column (Pharmacia) equilibrated in 50 mM Tris, pH 8.0, and 1 mM DTT. Bound protein was eluted with a linear salt gradient over 200 mL from 0 to 2 M NaCl. Protein was further purified by gel-filtration chromatography on either a G75 Sepharose or a G200 Sepharose HR26/60 column equilibrated in 50 mM Tris, pH 8.0, 150 mM NaCl and 1 mM DTT. The purity and identity of proteins was determined by SDS-PAGE and mass spectrometry.

Determination of oligomeric states of Hop and Hop truncations

Analytical SEC was performed on a Sephadex 200 HR10/30 (Pharmacia) column equilibrated in 50 mM, pH 8.0, 150 mM NaCl, 1 mM DTT and 10% glycerol. The relative elution volumes of 100 μL of sample containing between 3.5 and 100 μM Hop, Hop 1–222, Hop 1–352 and Hop 1–477 were compared with molecular mass standards (Sigma).

The relative elution volume was calculated as:

$$K_{AV} = \frac{V_e - V_0}{V_g - V_0}$$

where V_e is the elution volume and V_0 is the void volume determined by the elution of blue dextran 2000 (Sigma) and V_g.

Protein interaction assays

Protein interaction was assayed according to previously published protocols.[39] Samples (200 μL) containing 50 μM of the different proteins and protein complexes were incubated for 10 min at room temperature (25 °C) and 10 min on ice in 50 mM Tris, pH 8.0, 150 mM NaCl, 5 mM MgCl₂ and 1 mM DTT. Samples were separated on a Superose 12 HR 10/30 analytical column, pre-equilibrated in 50 mM Tris, pH 8.0, 150 mM NaCl, 5 mM MgCl₂ and 1 mM DTT at 4 °C on an ÄKTA Explorer™ system (Amersham-Biosciences). Fractions (100 mL) were collected, concentrated and analyzed by SDS gel electrophoresis.

Small angle X-ray scattering

SAXS data were collected at station 2.1 of the Daresbury SRS. Intensity of the incident X-rays was monitored by an ionization chamber installed in front of the sample, which was contained in a beam-line-specific standard sample cell. Protein concentrations of between 1 and 10 mg/mL were used. Reduction of the 2-D SAXS patterns of samples and corresponding buffers to 1-D scattering profiles was performed using established procedures. Data acquisition time was divided in frames of 60 s in order to monitor radiation damage (buffer and sample were measured in alternation). Sample-to-detector distances were configured so as to cover the low-angle region characterized by the momentum transfer interval of $0.002 \ \text{Å}^{-1} \leq s \leq 0.045 \ \text{Å}^{-1}$. The modulus of the momentum transfer is defined as

$s = 2\sin\theta/\lambda$; where 2θ is the scattering angle and λ the X-ray wavelength (1.54 Å). Reduction and analysis of 1-D scattering data sets were performed as previously described.[40] Radius of gyration, R_g, forward scattering intensity, I_0, and the intraparticle distance distribution function, $p(r)$, were calculated from the experimental scattering data using the indirect Fourier transform method as implemented in the program GNOM.[41] The maximum linear dimension, D_{max}, of the particle was evaluated according to the characteristic of $p(r)$. In order to check the consistency of the results, radii of gyration were also determined from the very low angle profiles by using the Guinier analysis based on the approximation:

$$\ln I(s) = \ln I_0 - 4\pi^2 R_g^2 s^2/3.$$

Particle shapes were restored from the experimental scattering profiles using the *ab initio* procedure based on the simulated annealing algorithm to a set of dummy spheres representing the amino acid chain of the protein (GASBOR).[42] Information from atomic models was exploited to define the nature of the observed scattering features in structural terms. Scattering curves were evaluated from these models using the program CRYSOL.[43] This method takes the solvent effect into account by surrounding the protein with a hydration shell of thickness 3 Å and of uniform density different from that of bulk solvent.

The structure of full-length Hop was obtained using the rigid-body modelling program BUNCH.[44] The dimerisation interface consisting of TPR2a was obtained by modeling the TPR2a (PDB ID code 1elr) domain onto the dimerisation interface of the GlcNac dimer (PDB ID code 1w3b).[26] Rigid-body modeling was carried out using the TPR1 domain of Hop (PDB ID code 1elw); structures for TPR2b, DP1 and DP2 domains were obtained using the Web-based structure prediction server Lomets.[25] Modelling was carried out assuming 2-fold symmetry around the conserved dimerisation interface at TPR2a (which was modeled based on the TPR domain interaction in the dimeric O-linked GlcNac transferase protein[26]).

Isothermal titration calorimetry

ITC was performed using a MicroCal VP-ITC instrument (MicroCal Inc., Northampton, MA). A total of 300 μL of 100 μM WT or mutant human Hsp90β was injected into a cell containing 8 μM Hop. In experiments looking at the effect of AMPPNP on Hop binding, saturating amounts of AMPPNP were calculated based on the K_d between WT and mutant Hsp90 and the nucleotide and added to the cell containing Hsp90. In the case of the A116N mutant, 200 μM protein was injected into 10 μM Hop due to the reduced affinity of this mutant.

Three hundred microliters of 600 μM WT Hsp90β, Hsp90C or SRMEEVD was injected into a cell containing 30 μM Cyp40 to measure the dissociation constants of binding for Cyp40, whilst 600 μM or 3.78 mM of Hsp90C and SRMEEVD, respectively, were injected into a cell containing 50 and 55 μM Hop, respectively, to measure the binding constants for Hop with various Hsp90 constructs.

All experiments were carried out in 50 mM Tris, pH 7.4, 6 mM $MgCl_2$, 20 mM KCl and 1 mM tris(2-carboxyethyl) phosphine at 25 °C. Parallel experiments were carried out in which injectant was added to buffer without protein to correct for the heat of dilution in subsequent data analysis using the Origin software package (MicroCal Inc.). Protein and nucleotide concentrations were determined spectrophotometrically.

References

1. Wegele, H., Muller, L. & Buchner, J. (2004). Hsp70 and Hsp90—a relay team for protein folding. *Rev. Physiol. Biochem. Pharmacol.* **151**, 1–44.
2. Pratt, W. B. (1997). The role of the Hsp90-based chaperone system in signal transduction by nuclear receptors and receptors signalling via MAP kinase. *Annu. Rev. Pharmacol. Toxicol.* **37**, 297–326.
3. Picard, D. (2002). Heat-shock protein 90, a chaperone for folding and regulation. *Cell Mol. Life Sci.* **59**, 1640–1648.
4. Young, J. C., Moarefi, I. & Hartl, F. U. (2001). Hsp90: a specialized but essential protein-folding tool. *J. Cell Biol.* **154**, 267–273.
5. Pearl, L. H. (2005). Hsp90 and Cdc37—a chaperone cancer conspiracy. *Curr. Opin. Genet. Dev.* **15**, 55–61.
6. Kamal, A., Thao, L., Sensintaffar, J., Zhang, L., Boehm, M. F., Fritz, L. C. & Burrows, F. J. (2003). A high-affinity conformation of Hsp90 confers tumour selectivity on Hsp90 inhibitors. *Nature*, **425**, 407–410.
7. Roe, S. M., Prodromou, C., O'Brien, R., Ladbury, J. E., Piper, P. W. & Pearl, L. H. (1999). Structural basis for inhibition of the Hsp90 molecular chaperone by the antitumor antibiotics radicicol and geldanamycin. *J. Med. Chem.* **42**, 260–266.
8. Obermann, W. M. J., Sondermann, H., Russo, A. A., Pavletich, N. P. & Hartl, F. U. (1998). *In vivo* function of Hsp90 is dependent on ATP binding and ATP hydrolysis. *J. Cell Biol.* **143**, 901–910.
9. Smith, D. & Toft, D. (1993). Steroid receptors and their associated proteins. *J. Mol. Endocrinol.* **7**, 4–11.
10. Scheufler, C., Brinker, A., Bourenkov, G., Pegoraro, S., Moroder, L., Bartunik, H. *et al.* (2000). Structure of TPR domain–peptide complexes: critical elements in the assembly of the Hsp70–Hsp90 multichaperone machine. *Cell*, **101**, 199–210.
11. Carrigan, P. E., Nelson, G. M., Roberts, P. J., Stoffer, J., Riggs, D. L. & Smith, D. F. (2004). Multiple domains of the co-chaperone Hop are important for Hsp70 binding. *J. Biol. Chem.* **279**, 16185–16193.
12. Flom, G., Weekes, J., Williams, J. J. & Johnson, J. L. (2006). Effect of mutation of the tetratricopeptide repeat and aspartate–proline 2 domains of Sti1 on Hsp90 signaling and interaction in *Saccharomyces cerevisiae*. *Genetics*, **172**, 41–51.
13. Chen, S. & Smith, D. F. (1998). Hop as an adaptor in the heat shock protein 70 (Hsp70) and hsp90 chaperone machinery. *J. Biol. Chem.* **273**, 35194–35200.
14. Nelson, G. M., Huffman, H. & Smith, D. F. (2003). Comparison of the carboxy-terminal DP-repeat region in the co-chaperones Hop and Hip. *Cell Stress Chaperones*, **8**, 125–133.
15. Johnson, J. L., Halas, A. & Flom, G. (2007). Nucleotide-dependent interaction of *Saccharomyces cerevisiae* Hsp90 with the cochaperone proteins Sti1, Cpr6, and Sba1. *Mol. Cell. Biol.* **27**, 768–776.
16. Flom, G., Behal, R. H., Rosen, L., Cole, D. G. & Johnson, J. L. (2007). Definition of the minimal fragments of Sti1

required for dimerization, interaction with Hsp70 and Hsp90 and *in vivo* functions. *Biochem. J.* **404**, 159–167.

17. Ali, M. M., Roe, S. M., Vaughan, C. K., Meyer, P., Panaretou, B., Piper, P. W. *et al.* (2006). Crystal structure of an Hsp90–nucleotide–p23/Sba1 closed chaperone complex. *Nature*, **440**, 1013–1017.

18. Prodromou, C., Panaretou, B., Chohan, S., Siligardi, G., O'Brien, R., Ladbury, J. E. *et al.* (2000). The ATPase cycle of Hsp90 drives a molecular 'clamp' via transient dimerization of the N-terminal domains. *EMBO J.* **19**, 4383–4392.

19. Pearl, L. H. & Prodromou, C. (2006). Structure and mechanism of the Hsp90 molecular chaperone machinery. *Annu. Rev. Biochem.* **75**, 271–294.

20. Koch, M. H., Vachette, P. & Svergun, D. I. (2003). Small-angle scattering: a view on the properties, structures and structural changes of biological macromolecules in solution. *Q. Rev. Biophys.* **36**, 147–227.

21. Odunuga, O. O., Longshaw, V. M. & Blatch, G. L. (2004). Hop: more than an Hsp70/Hsp90 adaptor protein. *Bioessays*, **26**, 1058–1068.

22. Lee, P., Shabbir, A., Cardozo, C. & Caplan, A. J. (2004). Sti1 and Cdc37 can stabilize Hsp90 in chaperone complexes with a protein kinase. *Mol. Biol. Cell*, **15**, 1785–1792.

23. Taylor, P., Dornan, J., Carrello, A., Minchin, R. F., Ratajczak, T. & Walkinshaw, M. D. (2001). Two structures of cyclophilin 40: folding and fidelity in the TPR domains. *Structure*, **9**, 431–438.

24. Ward, B. K., Allan, R. K., Mok, D., Temple, S. E., Taylor, P., Dornan, J. *et al.* (2002). A structure-based mutational analysis of cyclophilin 40 identifies key residues in the core tetratricopeptide repeat domain that mediate binding to Hsp90. *J. Biol. Chem.* **277**, 40799–40809.

25. Wu, S. & Zhang, Y. (2007). LOMETS: a local meta-threading-server for protein structure prediction. *Nucleic Acids Res.* **35**, 3375–3382.

26. Jinek, M., Rehwinkel, J., Lazarus, B. D., Izaurralde, E., Hanover, J. A. & Conti, E. (2004). The superhelical TPR-repeat domain of O-linked GlcNAc transferase exhibits structural similarities to importin alpha. *Nat. Struct. Mol. Biol.* **11**, 1001–1007.

27. Taylor, P., Dornan, J., Carrello, A., Minchin, R. F., Ratajczak, T. & Walkinshaw, M. D. (2001). Two structures of cyclophilin 40: folding and fidelity in the TPR domains. *Struct. Fold. Des.* **9**, 431–438.

28. Prodromou, C., Siligardi, G., O'Brien, R., Woolfson, D. N., Regan, L., Panaretou, B. *et al.* (1999). Regulation of Hsp90 ATPase activity by tetratricopeptide repeat (TPR)-domain co-chaperones. *EMBO J.* **18**, 754–762.

29. Carrigan, P. E., Sikkink, L. A., Smith, D. F. & Ramirez-Alvarado, M. (2006). Domain:domain interactions within Hop, the Hsp70/Hsp90 organizing protein, are required for protein stability and structure. *Protein Sci.* **15**, 522–532.

30. Song, Y. & Masison, D. C. (2005). Independent regulation of Hsp70 and Hsp90 chaperones by Hsp70/ Hsp90-organizing protein Sti1 (Hop1). *J. Biol. Chem.* **280**, 34178–34185.

31. Richter, K., Muschler, P., Hainzl, O., Reinstein, J. & Buchner, J. (2003). Sti1 is a non-competitive inhibitor of the Hsp90 ATPase. Binding prevents the N-terminal dimerization reaction during the ATPase cycle. *J. Biol. Chem.* **278**, 10328–10333.

32. McLaughlin, S. H., Smith, H. W. & Jackson, S. E. (2002). Stimulation of the weak ATPase activity of human hsp90 by a client protein. *J. Mol. Biol.* **315**, 787–798.

33. Siligardi, G., Hu, B., Panaretou, B., Piper, P. W., Pearl, L. H. & Prodromou, C. (2004). Co-chaperone regulation of conformational switching in the Hsp90 ATPase cycle. *J. Biol. Chem.* **279**, 51989–51998.

34. Travers, S. A. & Fares, M. A. (2007). Functional co-evolutionary networks of the Hsp70–Hop–Hsp90 system revealed through computational analyses. *Mol. Biol. Evol.* **24**, 1032–1044.

35. Lassle, M., Blatch, G. L., Kundra, V., Takatori, T. & Zetter, B. R. (1997). Stress-inducible, murine protein mSTI1. Characterization of binding domains for heat shock proteins and *in vitro* phosphorylation by different kinases. *J. Biol. Chem.* **272**, 1876–1884.

36. Chen, S., Prapapanich, V., Rimerman, R. A., Honore, B. & Smith, D. F. (1996). Interactions of p60, a mediator of progesterone receptor assembly, with heat shock proteins hsp90 and hsp70. *Mol. Endocrinol.* **10**, 682–693.

37. Hernandez, M. P., Sullivan, W. P. & Toft, D. O. (2002). The assembly and intermolecular properties of the hsp70–Hop–hsp90 molecular chaperone complex. *J. Biol. Chem.* **277**, 38294–38304.

38. McLaughlin, S. H., Ventouras, L. A., Lobbezoo, B. & Jackson, S. E. (2004). Independent ATPase activity of Hsp90 subunits creates a flexible assembly platform. *J. Mol. Biol.* **344**, 813–826.

39. Harst, A., Lin, H. & Obermann, W. M. (2005). Aha1 competes with Hop, p50 and p23 for binding to the molecular chaperone Hsp90 and contributes to kinase and hormone receptor activation. *Biochem. J.* **387**, 789–796.

40. Grossmann, J. G., Hall, J. F., Kanbi, L. D. & Hasnain, S. S. (2002). The N-terminal extension of rusticyanin is not responsible for its acid stability. *Biochemistry*, **41**, 3613–3619.

41. Svergun, D. I. (1992). Determination of the regularization parameter in indirect-transform methods using perceptual criteria. *J. Appl. Crystallog.* **25**, 495–503.

42. Svergun, D. I., Petoukhov, M. V. & Koch, M. H. (2001). Determination of domain structure of proteins from X-ray solution scattering. *Biophys. J.* **80**, 2946–2953.

43. Svergun, D., Barberato, C. & Koch, M. J. (1995). CRYSOL - a program to evaluate X-ray solution scattering of biological macromolecules from atomic coordinates. *J. Appl. Crystallogr.* **28**, 768–773.

44. Petoukhov, M. V. & Svergun, D. I. (2005). Global rigid body modeling of macromolecular complexes against small-angle scattering data. *Biophys. J.* **89**, 1237–1250.